A round jet in an ambient co-axial stream

By J. F. J. MACZYŃSKI

Department of the Mechanics of Fluids, University of Manchester†

(Received 20 December 1961)

Measurements were made of the mean velocity profiles in a jet immersed in a stream whose velocity was in the same direction as that of the jet. They showed a mean velocity on the jet axis falling inversely as the distance downstream of the jet origin, a behaviour demonstrably inconsistent with any theory which assumes that the turbulence at each section of the jet is in local equilibrium. A mixing length, L_M, and a length, L_d, characterizing the rate of dissipation are defined and it is shown that L_M increases with distance downstream more rapidly than the jet width, and L_d less rapidly.

1. Introduction

This paper is concerned with the flow of a turbulent jet emitted into a surrounding fluid having a uniform velocity in the same direction as the jet. The flow has some practical importance since it resembles that in ejector pumps and certain gas burners, but is also of considerable theoretical interest since it enables theories of jets to be tested much more stringently than does the flow of a jet into a stationary fluid when the form of the variation of jet width and velocity with distance can be predicted on dimensional grounds alone.

Nearly all theories of jets assume that the turbulence is in equilibrium at every cross-section; thus, for example, they may assume an eddy viscosity depending on the distance from the nozzle which is proportional to the product of the jet width and a characteristic velocity at that distance (Squire & Trouncer 1944). The measurements reported here are not consistent with this type of theory. It is found that the maximum excess velocity in the jet is closely inversely proportional to the distance from the jet nozzle over the whole range covered by the measurements (from where the excess jet velocity is much greater than that of the ambient stream to where it is much less), and it is shown by a detailed discussion of the order of magnitude of the terms in the equation for the turbulent energy balance that a consequence of this is that at large distances downstream the effective mixing length is proportional to the distance from the jet nozzle and not to the jet width which grows more slowly.

Previous measurements of compound jets have been made by Forstall & Shapiro (1950). In their equipment, however, the surrounding stream was contained in a pipe not very many times larger than the jet itself at large distances from the nozzle; so, although they found a velocity variation much the same as that in the present work, the disagreement with theory was not conclusive. Also

† Present address: Instytut Podstawowych Problemow Techniki, Krakow, Poland.

since the completion of the present work, the author has had his attention called to a brief paper by Kobashi (1952) which includes some measurements of turbulence in compound jets; these are completely consistent with the conclusions reached here.

2. Dimensional analysis of a jet in ambient flow

We shall ignore the initial portion of the jet where the shapes of the nozzle and velocity profile in the emergent jet have an appreciable influence on the flow, and consider only the region beyond this where the dynamic pressure distribution is found to be self-preserving, i.e. the shape of the profile is independent of downstream distance.

P_S and P_T are the static and total pressures relative to atmosphere, and q, equal to $P_T - P_S$, is the dynamic pressure which outside the jet takes the constant value q_A and on the centre line of the jet has the value q_C.

The experiments show that any profile of $q - q_A$ can be obtained from another by an appropriate change of scale, indicating a self-preservation of the excess dynamic pressure: except far downstream from the nozzle, this is not even approximately consistent with self-preservation of the excess velocity profile. Hence a characteristic value of the excess pressure, say $q_C - q_A$, and a characteristic length b, together with a function $g(r/b)$ are sufficient to describe any profile. Thus

$$q - q_A = (q_C - q_A)\, g(r/b). \tag{1}$$

These two characteristic profile parameters depend in turn on the distance x from the nozzle exit, on the mean exit velocity V_0, the nozzle diameter $2h_0$, and the velocity of the ambient stream U_A, so that on dimensional grounds,†

$$\frac{b}{h_0} = f_1(x/h_0,\, U_A/V_0), \tag{2a}$$

$$(q_C - q_A)/q_A = f_2(x/h_0,\, U_A/V_0). \tag{2b}$$

We now introduce a quantity B defined by

$$B = (U^2 - U_A^2)/U_A^2 = (q - q_A)/q_A, \tag{3}$$

and write B_C for its value on the jet centre line. Also for the sake of brevity we write H for the 'momentum radius' which by the principle of conservation of momentum is independent of x:

$$H = (M/\pi\rho U_A^2)^{\frac{1}{2}},$$
$$= \left(\int_0^\infty \left(\frac{U}{U_A} - 1\right) \frac{U}{U_A}\, 2r\, dr\right)^{\frac{1}{2}}, \tag{4}$$

where M denotes the momentum flux in excess of the ambient stream and U is the axial velocity component of the flow in the jet.

† Since we are concerned with fully developed turbulent flow at large Reynolds number, viscosity does not appear in our analysis (Townsend 1956).

The argument, which appears to be supported by experiment, that far enough downstream the jet nozzle may be considered as a point source of momentum, suggests that the nozzle radius h_0 and exit velocity V_0 are not separately important in this region but occur only in combination in H. Hence for large x, we may expect

$$\frac{b}{H} = f_3\left(\frac{x}{H}\right) \quad \text{and} \quad B_C = f_4\left(\frac{x}{H}\right). \tag{5}$$

Using the condition that the momentum flux is independent of x, a relation can be found between b/H and B_C for any function g. It is evaluated for a gaussian form of g in the Appendix.

Following Morton, Taylor & Turner (1956) we introduce the lateral spread of the jet h and the 'top-hat' mean velocity V, defined by the relations

$$Vh^2 = \int_0^\infty (U - U_A)\, 2r\, dr, \tag{6a}$$

$$V^2h^2 = \int_0^\infty (U - U_A)^2\, 2r\, dr. \tag{6b}$$

The mean values defined above can be understood to be the width and velocity in an equivalent jet with a sharp boundary and uniform velocity, $V + U_A$, carrying the same mass flow and excess momentum flux as the actual jet. Using V and h the main experimental problem is to find h/H and V/U_A as functions of x/H, where H is given by the relation

$$H^2 = \frac{V^2h^2}{U_A^2} + \frac{Vh^2}{U_A}. \tag{7}$$

The spread of the profile can be described by either of the two characteristic length scales b or h. For any particular form of the function g it is possible to derive a relation between b and h as shown in the Appendix (equations A 6 and A 8) for the gaussian profile.

3. The experimental arrangement

The experiments were performed in the low-turbulence tunnel of the Fluid Mechanics Laboratory at the University of Manchester, which has a working section 3 m long with a 50×50 cm cross-section. This tunnel was described in detail by Collis (1952).

The air speed in the tunnel is adjustable up to the top value of about 30 m/sec and the turbulence level is particularly low (about 0·04 %).

The jet outlet nozzle which was fitted in the tunnel by means of three sets of diagonal supporting wires consisted of a piece of 0·64 cm bore copper tube approximately 57 cm long. The tube was supplied with compressed air via a needle valve from three receivers each of 45 m^3 capacity. As a result of the discharge of air into the jet, the pressure in the reservoirs fell slowly during each experiment and it was necessary to adjust the needle valve setting with every reading. This, however, proved to be better than continuous pumping which introduced pressure fluctuations.

The dynamic pressure in the undisturbed flow which was needed to determine U_A was measured by means of a static tube and a total pressure tube fixed symmetrically with respect to the jet well outside it but beyond the influence of the tunnel-wall boundary layers.

Dynamic pressure in the jet was measured by means of a total pressure tube mounted on a traversing gear covering a large portion of the greatest jet spreads observed. The vertical position of the probe was determined to an accuracy of 0·01 cm by means of a telemicroscope mounted on a column. The corresponding accuracies in lateral and longitudinal position were 0·02 cm and 0·05 cm respectively.

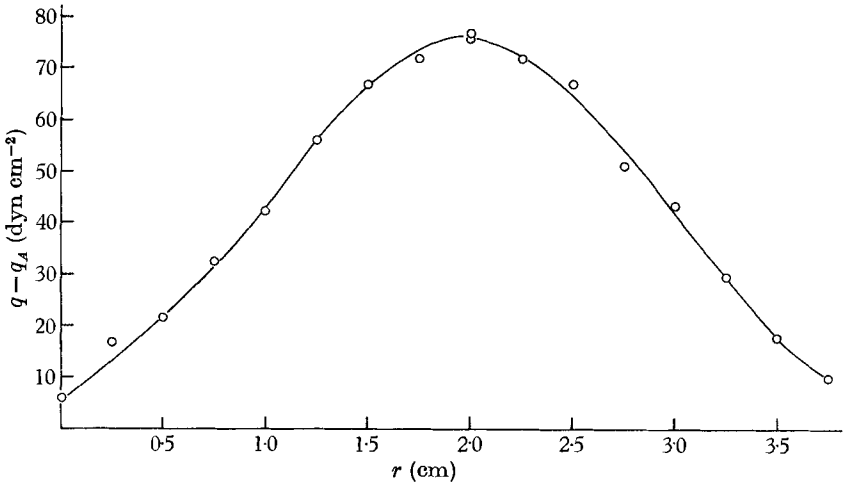

FIGURE 1. Shape of the jet pipe wake profile at 67 cm downstream and $q_A = 641$ dyn cm^{-2}.

The jet momentum flux was adjusted by controlling the pressure in the settling tank supplying the jet nozzle and was evaluated from actual Pitot traverses of the flow rather than from the supply pressure because of the long length of the nozzle tube and the uncertainty concerning the friction losses occurring in it. It is interesting to note that the nozzle discharge coefficient was found to be $0{\cdot}539 \pm 0{\cdot}013$ (as compared with 0·6 for a sharp orifice) and this provided a check against gross errors.

The presence of the long pipe upstream of the jet exit implies a departure from uniformity in the surrounding flow. A measure of the seriousness of this is given by the ratio of the drag on the pipe due to the external stream, D, to the excess momentum flux in the jet, M. From the definition of the momentum radius (4) and a similar expression for the drag radius H_D, this ratio can be written as

$$\frac{D}{M} = \left(\frac{H_D}{H}\right)^2.$$

The drag radius was found from a wake traverse (figure 1) at 67 cm from the nozzle, with no jet, to be 0·28 cm when q_A was 641 dyn/cm^2. This value is from one-thirtieth to one-sixth of H, therefore D/M varied from 3 % to 0·1 % in the range covered by the experiments.

As an indication of the accuracy of the pressure measurements in the jet, the momentum radius deduced from them was found to be independent of x to an accuracy of 2 %.

4. The experimental results

The shape of the dynamic pressure profile

The values of dynamic pressure were corrected for the static pressure defect, which was found to be of the order of 1 % at the centre of the jet. Four profiles of the dynamic pressure $(q-q_A)$ representing traverses near the nozzle and far downstream are shown on figure 2. They are replotted on figure 3 where the vertical scale is the logarithm of $q-q_A$ and the horizontal scale is the square of the distance from the centre line, so that if a profile of $q-q_A$ were gaussian it would be represented on the graphs by a straight line.

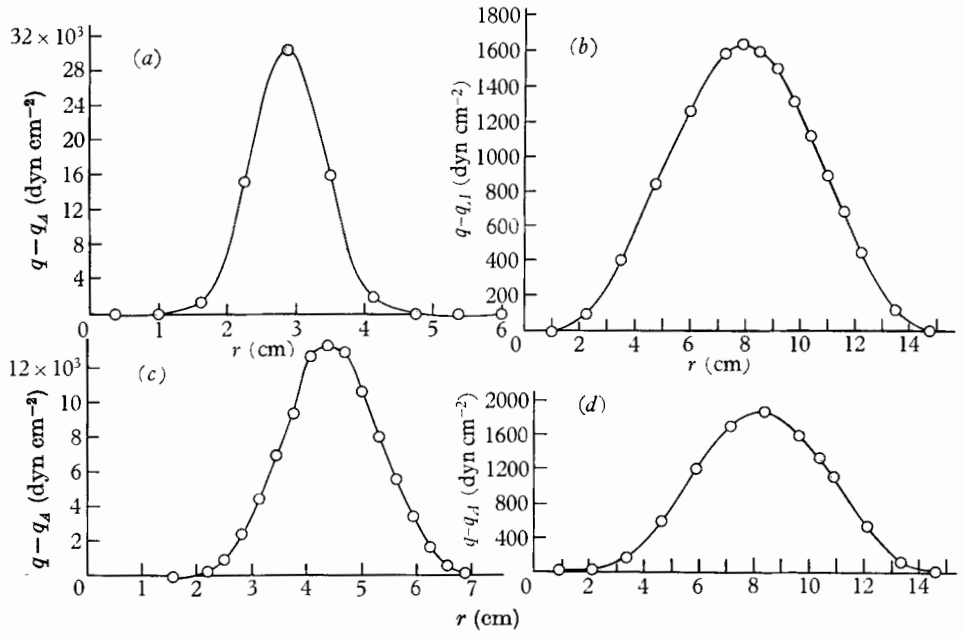

FIGURE 2. Shape of the total pressure profiles $(q-q_A)$ for pressures before jet nozzle $P_J = 0{\cdot}491\times10^6$ dyn cm^{-2}. Curve (*a*) 16·8 cm from the nozzle, $q_A = 5670$ dyn cm^{-2}; curve (*b*) 108·2 cm from the nozzle, $q_A = 2570$ dyn cm^{-2}; curve (*c*) 24·18 cm from the nozzle, $q_A = 2600$ dyn cm^{-2}; curve (*d*) 133·5 cm from the nozzle, $q_A = 5759$ dyn cm^{-2}.

It is seen that near the centre of the jet the profiles follow the gaussian form but that near the edge they fall off with distance somewhat more steeply. This deviation is found consistently and cannot be attributed to experimental error. It is probably associated with the radial inflow into the jet which inhibits turbulent spreading and is most important in the outer part for two reasons. First of all the lateral inflow changes sign when we proceed from the centre line outwards and has therefore the opposite effect in the central part of the jet. Furthermore it is where the axial flow induced by the jet is weakest that the effect of lateral inflow on the spreading is most pronounced.

Axial variation of the mean flow

The range of values of B_C covered in the experiments was from 0·339 to 21·0 and was achieved by making measurements at several values of x using various combinations of jet exit velocity and tunnel speed.

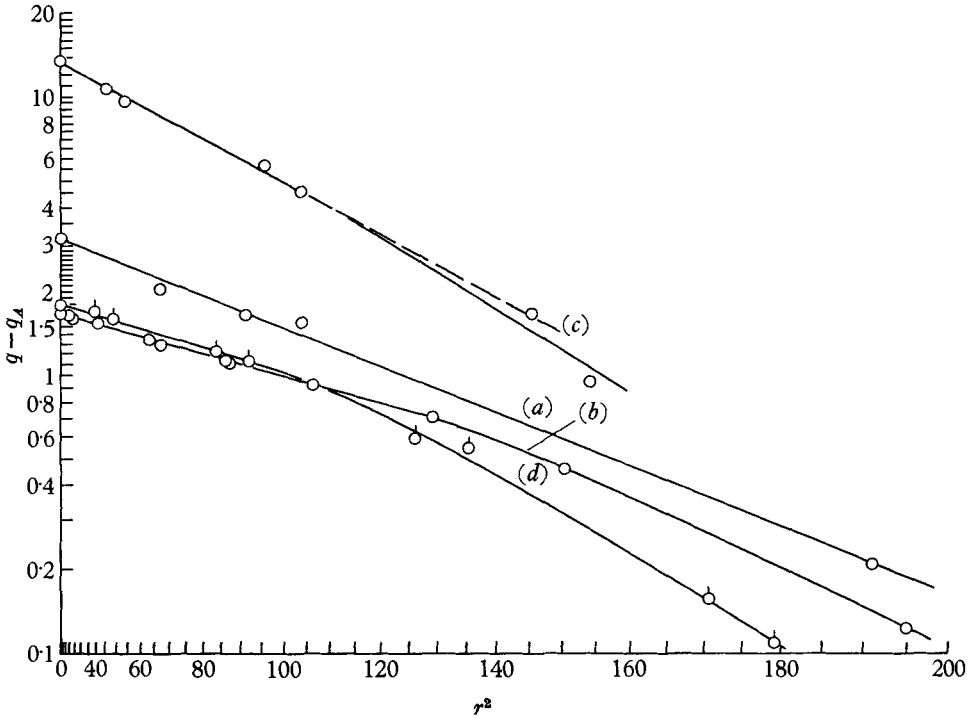

FIGURE 3. Plots of curves (*a*), (*b*), (*c*) and (*d*) from figure 2 as $\log(q-q_A)$ *vs* r^2 with arbitrary proportional scales.

The momentum radius H was found from equation (A 4) of the Appendix using values of b obtained from plots of $\log B$ against r^2. B_C^{-1} was then plotted against x/H as shown on figure 4. A smooth curve obtained from these points was used to compute h/H, V/V_0 and Vx/V_0h_0 as functions of x/H; these are shown in figure 5.

The relation
$$0{\cdot}144Vx/V_0h_0 = 1 \tag{8}$$
can be regarded as a convenient summary of the measurements together with the approximately gaussian shape of the profiles.

The form of the variation of h with x may be calculated from (8) and (7).
$$h = 0{\cdot}144x(1+0{\cdot}144x/H)^{-\frac{1}{2}}, \tag{9}$$
which at small x/H reduces to the linear spread known for a jet in still air. Hence
$$\frac{dh}{dx} = 0{\cdot}144(1+0{\cdot}072x/H)\,(1+0{\cdot}144x/H)^{-\frac{3}{2}}, \tag{10}$$
which shows that the rate of increase of the jet radius tends to a constant when x/H tends to zero and to zero when x/H tends to infinity.

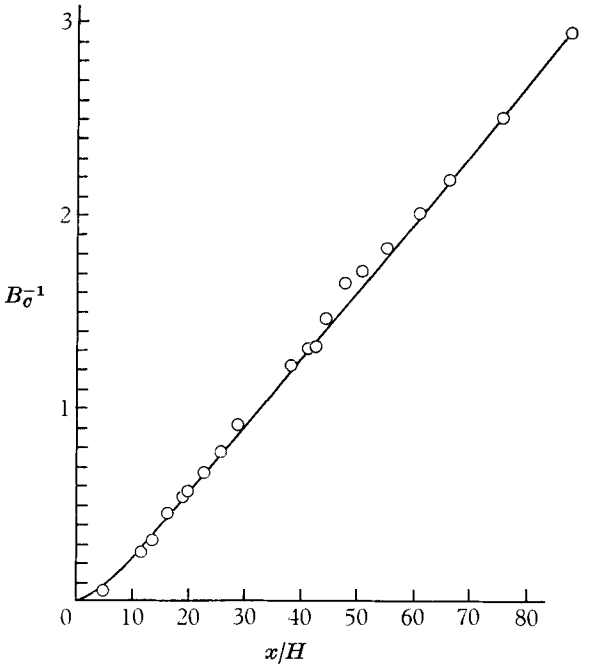

FIGURE 4. The variation of centre line excess pressure coefficient B_0 with dimensionless distance downstream x/H.

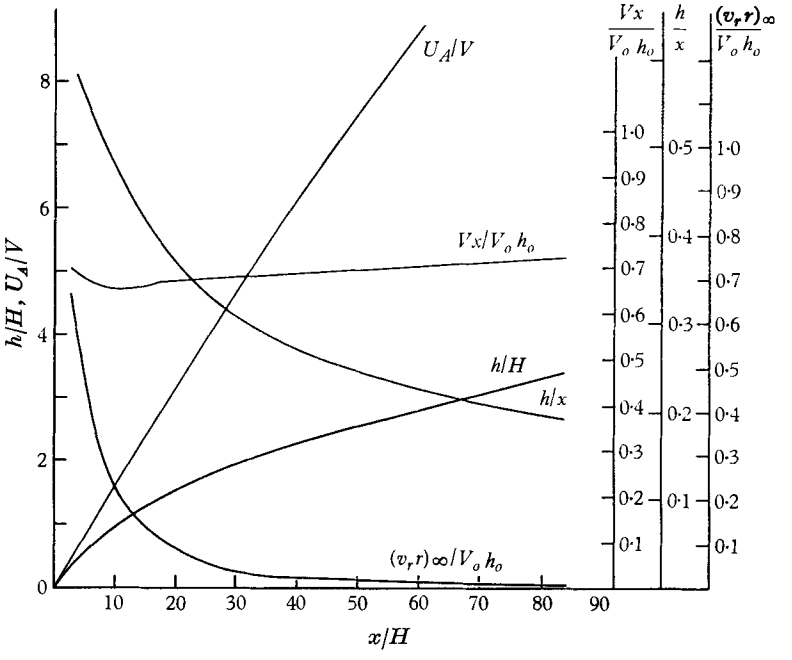

FIGURE 5. Dimensionless 'top-hat' mean velocity V/U_A, jet spread h/H, jet ratio h/x, lateral influx $(v_r r)_\infty/V_0 h_0$, as functions of x/H.

The lateral influx

The variation of the lateral influx appears to be an important feature distinguishing jets with and without ambient streams. For the sake of brevity we can characterize the lateral inflow by the dimensionless quantity $-v_r r/Vh$, where $v_r r$ is the product of the radial velocity component and the radius measured from the jet centre line. We are concerned here with the limit of this product at large r.

The equation of continuity,

$$\frac{\partial U}{\partial x}+\frac{1}{r}\frac{\partial (v_r r)}{\partial r}=0, \tag{11}$$

together with (3) yields

$$\begin{aligned}(v_r r)_{r=\infty} &= -\frac{U_A}{2}\frac{\partial}{\partial x}\int_0^\infty \frac{U}{U_A}\,2r\,dr \\ &= -\frac{U_A}{2}\frac{\partial}{\partial x}\int_0^\infty [(1+B)^{\frac{1}{2}}-1]\,2r\,dr. \end{aligned} \tag{12}$$

Or, making use of the definitions (6*a*) and (6*b*) and momentum equation (cf. Appendix equation (A 3)), we obtain

$$\frac{(v_r r)_{r=\infty}}{V_0 h_0} = -\tfrac{1}{2}H\frac{d}{dx}\left(\frac{1}{1+V/U_A}\right), \tag{13}$$

which according to the velocity decay relation (cf. equation 8) becomes

$$\frac{(v_r r)_{r=\infty}}{V_0 h_0} = -0{\cdot}072(1+0{\cdot}144x/H)^{-2}. \tag{14}$$

This may be written as

$$\frac{(v_r r)_{r=\infty}}{Vh} = -0{\cdot}072(1+0{\cdot}144x/H)^{-\frac{3}{2}}, \tag{15}$$

by virtue of (9).

Equation (15) shows how the lateral inflow $-(v_r r)/Vh$ falls from the constant value 0·072, appropriate to jet in a fluid at rest, to zero at large distances downstream of the orifice, characteristic of a wake. The total rate at which ambient fluid is entrained is made up from a combination of the lateral (jet-like) inflow and encroachment of the jet boundary on the ambient flow, as in a wake. Accordingly it is given by

$$\begin{aligned} d(Vh^2)/dx + U_A\, d(h^2)/dx &= (d/dx)\,(V+U_A)\,h^2, \\ &= 0{\cdot}144\,Vh\{1+0{\cdot}144(x/H)\}^{\frac{1}{2}}. \end{aligned} \tag{16}$$

5. Discussion

The relation (8) which has been found for the variation of V with x is not what would be expected from any simple theory which assumes that the rate of mixing at any cross-section of the jet is determined only by V and h at that cross-section and is independent of the history of the motion. Indeed in its simplest form such a theory would assume that the entrainment coefficient defined by

$$E=\frac{1}{2Vh}\frac{d}{dx}[(U_A+V)\,h^2] \tag{17}$$

would be a constant throughout the motion. Equation (16) shows that this is not even approximately so. That E should increase between the initial region of the jet where $B_C \gg 1$ and the region far downstream where $B_C \ll 1$ is not very surprising since in the initial region the inflow velocity is large and may tend to inhibit mixing, while far downstream it is small and the flow is more like that of a wake which is known to have a greater value for the entrainment constant (cf. Townsend 1956).

However, on this argument alone one would expect E to become asymptotically constant far downstream, where the wake-like character is achieved; but there is no sign of this happening.† It therefore seems worthwhile to examine briefly the asymptotic behaviour of the various terms in the equation of motion in the hope of learning more about the mechanism of the flow. It is

$$U\frac{\partial U}{\partial x}+v_r\frac{\partial U}{\partial r}=-\frac{1}{\rho}\frac{\partial p}{\partial r}+\frac{1}{\rho}\frac{\partial \tau}{\partial r}. \tag{18}$$

From equations (8) and (9) the V and h are seen to behave like x^{-1} and $x^{\frac{1}{2}}$ respectively when $x \to \infty$. The first term in the equation of motion thus behaves as

$$U\,\partial U/\partial x \sim U_A\,dV/dx = O(x^{-2}).$$

From the continuity equation,

$$v_r r = \int_0^r \partial U/\partial x\, r'\,dr' = O(h/x)^2 = O(x^{-1})$$

if we follow a line $r/h = \text{const}$.

Therefore the second term in (18) becomes

$$v_r\,\partial U/\partial r = O(x^{-1})\,O(x^{-\frac{1}{2}})\,O(x^{-1})\,O(x^{-\frac{1}{2}}) = O(x^{-3}),$$

which is less than the first term.

The pressure term vanishes, since there is no pressure gradient in an unbounded jet. The Reynolds stress term must adjust itself to fit the first term of the equation of motion, and $$\partial\tau/\partial r = O(\tau/h) = O(\tau x^{-\frac{1}{2}}) = O(x^{-2}).$$

Hence $$\tau = O(x^{-\frac{3}{2}}).$$

At the same time since the velocity gradient

$$\partial U/\partial r = O(x^{-\frac{3}{2}}),$$

the mean eddy viscosity becomes

$$K_M = \tau/(\partial U/\partial r) = O(x^0) = \text{const}. \tag{19}$$

A length L_M may be defined by $K_M = u'L_M$, where u' is characteristic of the turbulent velocity. It is obvious that for $u' = O(V) = O(x^{-1})$, L_M is $O(x)$ and not $O(h)$ as a spreading dependent on purely local flow properties at a cross-section would suggest. If more generally we assume that

$$u' = O(x^{-a}), \tag{20}$$

and

$$L_M = O(x^a), \tag{21}$$

† It is true that the minimum excess velocity measured was roughly 10 % of the main stream velocity and may still be rather too large for the asymptotic wake state to have been reached, but one would expect to have found a trend towards it.

and consider the turbulent energy balance in the flow it is seen that (*a*) the rate of production of turbulent energy is $O(h^2\tau\,\partial U/\partial r) = O(x^{-2})$; (*b*) if the dissipation of this energy involves a length $L_d = O(x^c)$, the total rate of dissipation per unit length of jet is

$$O(h^2 u'^3/L_d) = O(x^{1-3a-c});$$

(*c*) the rate of change of total turbulent energy is

$$O\left(\frac{d}{dx}(u'^2h^2)\right) = O\left(\frac{d}{dx}(x^{1-2a})\right) = O(x^{-2a}), \quad \text{if } a \neq \tfrac{1}{2}.$$

The order of magnitude equation of turbulent energy balance may thus be written as

$$O\{d(u^2h^2)/dx\} = -O(h^2u^3/L_d) + O(h^2U/r), \tag{22}$$

which for $a \neq \frac{1}{2}$ is equivalent to

$$-O(x^{-2a}) = -O(x^{1-3a-c}) + O(x^{-2}). \tag{23}$$

The signs are preserved since they convey the behaviour of the terms more explicitly.

Since the flow region increases in size with increasing x it seems plausible that L_d should either grow with x or remain constant, a decrease being improbable. Hence $c \geqslant 0$.

The three exponents $-2a$, $1-3a-c$, -2 may be either (i) all three equal with $a = 1$, $c = 0$ (this is when all three terms in the turbulent energy balance are of equal order of magnitude); or (ii) two of the three are equal and the third is smaller, which means that one term decays more rapidly than the others.

Alternative (ii) shows that there are three relations possible between c and a. These are: (*a*) $c = 1-a$, with $a \neq \frac{1}{2}$ which corresponds to the rate of production of turbulent energy becoming negligible; (*b*) $a = 1$, implying negligible dissipation. This case is excluded because the dissipative term must be the controlling term if the equation is to be balanced, the other two terms being of the same sign; (*c*) $c = 3(1-a) < 0$ which occurs for $a > 1$, and corresponds to production and dissipation dominating the energy balance. This possibility must be ruled out since $c \geqslant 0$.

We are left thus with $c = 1-a$ and the isolated possibility $a = \frac{1}{2}$, $c = \frac{3}{2}$ (for constant total turbulent energy).

Clearly extensive measurements of the turbulence are required to elucidate the mechanism of the flow. A few preliminary measurements of turbulent intensity have been made. They are plotted on figure 6 which shows the ratio of the R.M.S. turbulent velocity at the jet centre line to V as a function of x/H. This ratio appears to be approximately constant, consistent with $a = 1$, $L_M = O(x)$ and $L_d =$ constant, indicating that all three terms in (19) are of comparable order of magnitude.

The surprising implication of the above result is that neither of the two length scales required to describe the broad features of the jet turbulence is proportional to the width of the jet; the mixing length L_M increases more rapidly than h and the dissipation length L_d less rapidly.

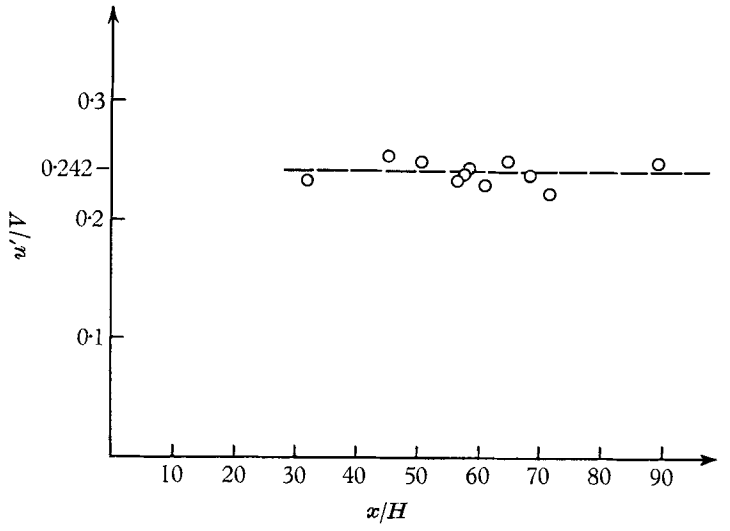

FIGURE 6. The ratio of the measured R.M.S. turbulence velocity u' to the mean top-hat excess velocity V for variable x/H.

The author wishes to express his gratitude to all who helped him to work on the problem and in particular to Professor P. R. Owen and Dr T. H. Ellison for helpful guidance, encouragement and important suggestions, and to the British Council for granting a scholarship.

REFERENCES

COLLIS, D. C. 1952 The dust problem in hot wire anemometry. *Aero. Quart.* **4**, 93.

FORSTALL, W. JR. & SHAPIRO, A. H. 1950 Momentum and mass transfer in co-axial gas jets. *J. Appl. Mech.* **72**, 399.

KOBASHI, Y. 1952 Experimental studies on compound jets. *Proc. 2nd Japan Nat. Congr. Appl. Mech.* pp. 223–6.

MORTON, B. R., TAYLOR, G. I. & TURNER, J. S. 1956 Turbulent gravitational convection from maintained and instantaneous sources. *Proc. Roy. Soc.* A, **234**, 1–23.

SQUIRE, H. B. & TROUNCER, J. 1944 Round jets in a general stream. *Aero. Res. Counc., Rep. & Memo.* no. 1904.

TOWNSEND, A. A. 1956 *The Structure of Turbulent Shear Flow.* Cambridge University Press.

Appendix

Consider the gaussian form of the dynamic pressure profile B.

$$B = B_C(x) \exp\left[-r^2/b^2(x)\right]. \tag{A 1}$$

Since by definition the velocity ratio U/U_A is given by (4),

$$U/U_A = (1+B)^{\frac{1}{2}}, \tag{A 2}$$

the expression for the total momentum flux is

$$M = \rho_0 \pi \int_0^\infty (U^2 - UU_A)\, 2r\, dr = 2P_A \left\{ \int_0^\infty B 2r\, dr - \int_0^\infty \left[(B+1)^{\frac{1}{2}} - 1\right] 2r\, dr \right\} \tag{A 3}$$

which integrated yields:

$$M = 2P_A b^2\{B_C - 2[(1+B_C)^{\frac{1}{2}} - 1 - \ln \tfrac{1}{2}((1+B_C)^{\frac{1}{2}}+1)]\}. \tag{A 4}$$

The above formula can be used to compute the momentum radius H (cf. equation (4)).

$$H = b[B_C - 2\beta(B_C)]^{\frac{1}{2}} = b[B_C - 2\beta_C]^{\frac{1}{2}}, \tag{A 5}$$

where β is introduced for the square bracket in (A 4).

Expressing the non-dimensional characteristics of the jet flow as functions of the excess pressure coefficient on the axis the following relations are obtained:

$$\left(\frac{h}{H}\right)^2 = \frac{4\beta_C^2}{(B_C - 4\beta_C)(B_C - 2\beta_C)}, \tag{A 6}$$

$$\frac{V}{U_A} = \frac{B_C - 4\beta_C}{2\beta_C}, \tag{A 7}$$

$$(b/H)^2 = (B_C - 2\beta_C)^{-1}. \tag{A 8}$$